CHAPTER 18

PERIODIC THEORY VELOCITY PREDICTION IN RANDOM WAVE

by John H. Nath[1], F.ASCE and Koji Kobune[2]

Abstract

Large waves in a series of random ocean waves are considered in the design of ocean structures. When random structural vibrations can be ignored, periodic wave theories are used to predict the water particle kinematics for a design wave even though the real wave is irregular. This paper presents the authors' first attempt to quantify the validity of using periodic wave theory for random waves. Measurements of maximum horizontal and vertical velocities were made in laboratory generated periodic and random waves. They compared favorably with predictions from periodic wave theories (even with Airy theory) particularly for the large waves in a series. Since the design wave concept is applied to the largest waves, the conclusion is that periodic wave theory may be adequate, providing an appropriate factor of safety is used to account for the differences between the actual maximum wave kinematics in nature and those in the predictive theory.

1.0 INTRODUCTION

Presented herein is a part of a continuing program of study at Oregon State University to determine the wave kinematics and dynamics in a closed system wave flume with experimentation and theory. Mass transport is also being studied and a first report on that subject is included in (8). For example, it is known that in wave flumes circulation patterns of mass transport must occur, the configurations of which are time dependent. How much these circulations affect the waves, and thus the experiments which depend on them, is not yet known. However, in the region in which measurements were made for this study, it is felt that the influence of circulation within the flume was small. Therefore, it was assumed to be negligible.

1.1 Purpose and Scope

The purpose of the work was to make measurements of water particle kinematics in individual random waves and to compare the results with predictions from periodic wave theory. The scope of the work included measurements of the maximum horizontal velocities under the crests and troughs of periodic and random waves and the vertical velocities at approximately the nodes. These measurements are compared with theoretical predictions and the errors are examined statistically. We estimate that the random waves in the laboratory have characteristics that are close enough to real ocean waves that the results can be applied to design conditions.

At least two methods have been developed to represent random ocean waves for the prediction of wave forces on marine structures. One is the conventional method which uses the design wave concept designated by

[1]Professor and Director of Environmental Fluid Dynamics Laboratory, Oregon State University, Corvallis, Oregon 97331, USA.

[2]Chief, Storm Surge and Tsunami Laboratory, Hydraulic Eng. Division, Port and Harbour Research Institute, Japan.

height (H_D) and period (T_D) and direction. The other utilizes the mean square spectral density of the water surface fluctuation which is herein called the wave spectrum. The latter method is important for the dynamic analysis of marine structures, such as relatively flexible offshore oil facilities. Short, stiff offshore oil facilities and massive structures, such as sea walls and breakwaters, are not very dynamically responsive to the waves and can, therefore, be treated with the design wave approach. The dynamic stability and fatigue characteristics of relatively flexible structures should be examined against the continuous random wave action. However, stiff structures can be designed as if the maximum wave loads are applied in a static manner.

The design wave technique includes considerations for the water depth, h, the wave height, H, and the period, T, which are determined on the basis of a statistical study. Wave records, hindcasting, experience and judgment are utilized. The design wave height is usually a large, rare value, and is sometimes specified as the "one hundred year wave" or something analagous thereto. The design wave should be defined as the largest wave to which the structure is likely to be subjected in its lifetime. On the other hand, the probability distribution of wave magnitudes can be estimated for a site for the lifetime of the structure and the design decision is focused on selecting a probability level beyond which the chances of having a higher wave are very small. The wave size at this probability level then becomes the design wave.

The water kinematics within such a wave are estimated by fitting a periodic wave to the profile and using an appropriate periodic wave theory. However, the design wave in nature will have an irregular profile and the kinematics may be different from those for a periodic wave.

Thus, the purpose of this study can be restated to be to examine the validity of using periodic wave theory for the design wave method, by estimating the error to be expected when a periodic wave theory is used to predict the water kinematics within a particular random wave.

1.2 Literature Review

Because of the difficulty of making Eulerian measurements of water particle velocities, few experimental studies on water kinematics of *random* waves have been reported.

Iwagaki, et. al., (4) measured water particle velocities of random waves utilizing a sonic doppler current meter. They found that Reid's numerical filter (9), i.e. superposition of many sinusoidal component waves, provided a fairly good estimate of the time series of water kinematics for a given time series of water surface elevation. Their velocity measurements showed that the horizontal velocity variation closely followed the water surface elevation, where the maxima and minima appeared at the wave crests and troughs, respectively, even in random waves. The vertical velocity was related to the slope of the water surface, and the peak vertical velocity occurred when the water surface crossed the still water level. The frequency response function for velocities was computed. The measured response functions turned out to be larger than the predicted response function for the high frequency range. They commented that such a difference was partly caused by the noise from the sonic doppler current meter.

Tsuchiya and Yamaguchi (10) measured the velocity of wind generated waves in a recirculation wave tank utilizing the sonic doppler current meter. They also noted the contamination of their record by the noise from the current meter.

The discussion about the water particle velocities of discrete waves in random waves is seen in the study by Grace and Rocheleu (2). They measured the near bottom velocities with a propeller meter beneath the wave crests and troughs of long period waves (from 14 to 20 seconds) simultaneously with the dynamic pressure at Waikiki Shore, Hawaii. For this wave period range and water depth (10.6 m), there was almost a constant ratio of the horizontal velocity beneath a wave crest, u_+, to the wave height deduced from Airy theory, H_p. The wave heights were defined as the average of the trough to crest height fore and aft the crest. Thus, their definition is different from the zero upcrossing wave height. The residuals between measured and predicted velocities were examined. The distribution turned out to be normal with a mean of -0.18 cm/sec and the standard deviation of 7.25 cm/sec. From the above discussion, they concluded that Airy theory provided an excellent prediction of the velocity beneath the wave crests.

Lee, et. al., (7) recently tested laser doppler anemometers in random wave action and they reported that it was a highly suitable instrument for laboratory study of waves. A full discussion about the kinematics, however, was not given in the paper.

2.0 METHOD

The methods used to meet the objectives are briefly presented, beginning with a condensed review of error sources.

2.1 Errors

In an experimental study of this kind, there are many sources of error between predictions and actual forces experienced by the structure. Some very important sources are:

1. Antiseptic conditions in the laboratory are considerably different than the conditions in the ocean. Wind driven ocean waves can be short crested and generally variable in many respects. The waves in this study were strictly two-dimensional. Wave theories assumed the waves are long crested and it is helpful to have laboratory waves modeling such conditions in order to corroborate the predictions.

2. Experimental errors can be minimized with proper calibration procedures. The natural frequencies of the measurement systems should be much higher than the frequencies of the items being measured. This study increased the reliability of the measurements by using two different instruments, a hot film anemometer and a small propeller meter. In addition, the signal to noise ratio should be on the order of 10:1 for precise measurements.

3. Innate errors in the wave theories contribute to overall errors. Since perfect measurements are not possible, it can only be said that results from the laboratory reflect the differences between theory and measurements as determined within the accuracy limits of the measurements. Often errors in theory are increased because theories are used in regions between the wave trough and wave crest even though boundary conditions

are established at the still water surface. It is not possible to find absolute errors in such cases.

4. Reflections from the beach can modify results, particularly for random waves. In order to get representative samples of waves, long periods of time are used. For this study the wave absorber was a concrete beach with a 1:12 slope which fairly well dissipated the wave energy. From previous experience, reflection coefficients range from 3% to 12% for wave periods of 1 to 5 secs. In addition, for long periods of testing, certain mass transport circulations must be established in the flume as previously mentioned. Such mass transport circulations cannot be adequately evaluated at this time.

2.2 Wave Theories

Three wave theories are employed to predict the maximum and minimum velocities -- Airy theory, which is simple and widely used for design of marine facilities; Stokes' fifth order theory; and Dean's Stream Function theory. Dean (1) showed that Stokes' fifth order theory is accurate for deep and near deep water wave conditions, and that Dean's Stream Function theory covers deep, intermediate and near shallow water wave conditions. The comparison was based on how well the theory predicted the kinematic and dynamic free surface boundary conditions. Mostly, deep water waves were tested for this work and there is no real difference between the predictions from Stokes' fifth order theory and those from Dean's Stream Function theory.

2.3 Laboratory Arrangement and Procedures

2.3.1 Facilities and instruments

The experiments were conducted in the Wave Research Facility at Oregon State University which is shown in Fig. 1. The wave tank is 104 m long, 3.7 m wide and 4.6 m deep. The wave absorber is a concrete beach with a slope of one on twelve. The wave generator has a flap-type wave board. The wave board is driven by a hydraulic piston which is controlled by an electric input, which can be either a sinusoidal or random signal. Additional information can be found in (3,8).

Fig. 1 Elevated View of OSU Wave Research Facility

The water surface elevation was measured with a Sonic System Model 86 sonic wave profiler. The velocities were measured with a Nover Nixon Streamflo Probe 403 propeller current meter and a Thermo Systems, Inc. (TSI) 1240-60W X-type cylindrical hot film anemometer, which are shown in Figs. 2 and 3.

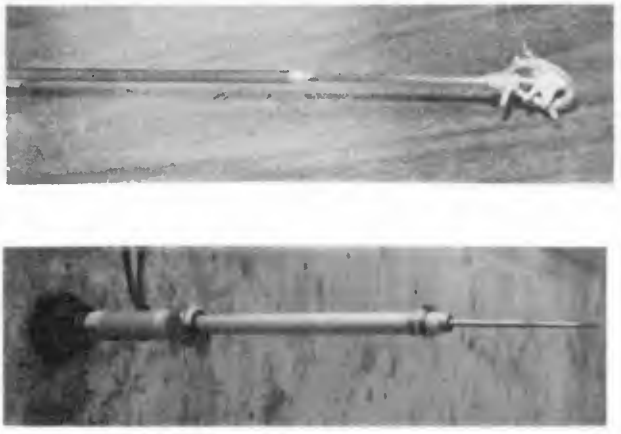

Fig. 3 Hot Film Anemometer Probe

The hot film probe was coupled with TSI model 1050 constant temperature anemometer and model 1052 linearizers. These probes were installed on the side walls of the wave tank as shown in Fig. 4.

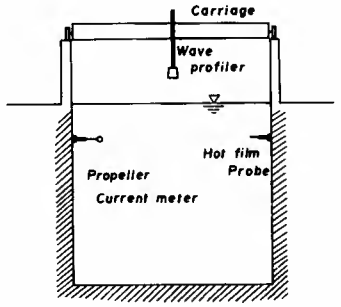

Fig. 4 Probe Set-up Looking North

The propeller probe has a diameter of 1.2 cm and is composed of five blades. When the propeller revolves, the passage of a blade past a gold wire tip, contained in the head of the slim support of the propeller, generates an electric pulse. The hot film probe has an orthogonal pair of quartz coated cylindrical hot film sensors with diameter of 0.15 m and sensing length of 2.0 mm. The sensors were operated at a low overheating ratio of 1.03 throughout the measurements, in order to avoid the generation of air bubbles on the sensor surface, which reduces the sensitivity. It was oriented in the waves as shown in Fig. 5.

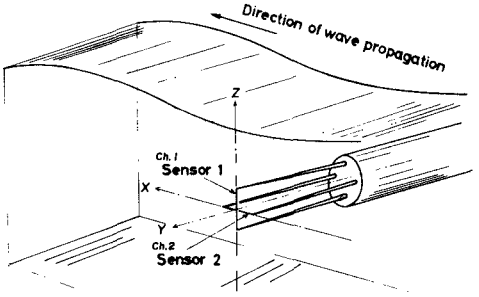

Fig. 5 Hot Film Anemometer Orientation

The hot film output voltage was linearized with a device which approximates the relation between the nonlinear output voltage, E_B, and the flow speed, V, by a fourth order polynomial. Thus, the relation of the linearized output voltage, E, to the flow speed, V, is expressed by the following equation:

$$E = A(\theta)\ V \tag{1}$$

where $A(\theta)$ is the directional function for the linearized output voltage, which is determined through calibration; and it takes a maximum when the yaw angle θ is zero, i.e., when the flow direction is perpendicular to the sensor axis and decreases according to the increase of θ, up to 90^o. As shown in Fig. 5, Sensor 1 was most sensitive to the horizontal velocity component, while Sensor 2 was most sensitive to the vertical velocity component. For data reduction, the maximum value in the time variation of the linearized output was processed using the calibration coefficient $A(0)$.

2.3.2 Calibration procedure

Calibration procedures are described in detail in (6) and reviewed briefly here. The primary calibration was conducted by swinging each probe in still water at the bottom of a long pendulum, which generated a damped free oscillation. Figure 6 illustrates the pendulum and Fig. 7 shows a typical output from the propeller meter. The hot film output was equally accurate, but continuous. The pendulum motion was monitored with a sonic sensor turned sideways and beamed to the reflector shown in Fig. 6. The range of the period of the pendulum motion was set from two to three seconds. The significant wave periods of the test random waves fall into this range.

The number of impulses per second from the propeller meter was calibrated from the pendulum motion for what is herein termed the low speed range. For speeds greater than about 9 cm/sec, the calibration curve fell on a straight line as shown in Fig. 8, where V_{max} is taken from the maxima of the pendulum velocities. It was also calibrated from a hand oscillated carriage, the motion of which was carefully monitored with the sonic sensor. The results are shown in Fig. 9 with the best fit straight line from Fig. 8 superimposed. The effects from nonalignment of the axis with the water flow direction was also examined

and found to be appreciable (6). Thus, only the horizontal wave velocities at the crests and troughs were considered with the propeller meter, as well as vertical velocities at the zero crossings.

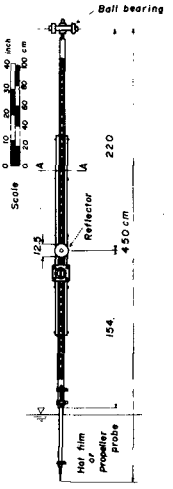

Fig. 6 Pendulum Calibration for Hot Film Anemometer

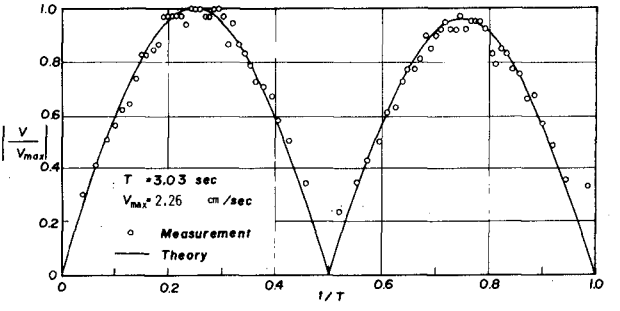

Fig. 7 Response of Propeller Current Meter

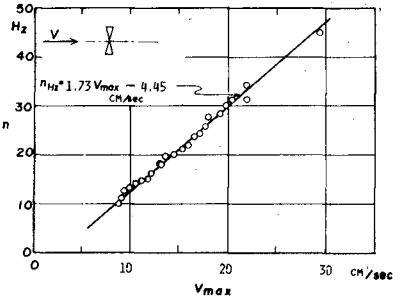

Fig. 8 Calibration of Propeller Current Meter for Low Speed Range

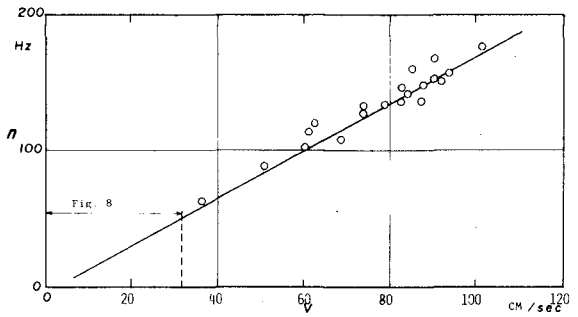

Fig. 9 Calibration of Propeller Current Meter for High Speed Range

The sensitivity of the hot film sensor is easily affected by dirt and fluid temperature. Therefore, the hot film anemometer was calibrated at the beginning and the end of each series of runs. In the case that these two calibrations were different, but not too different, the first half of the run was processed using the result of the calibration at the beginning, while the latter half was processed using the result at the end. A calibration example is shown in Fig. 10 where the plotted gage readings are for the velocity maxima, as with the propeller gage.

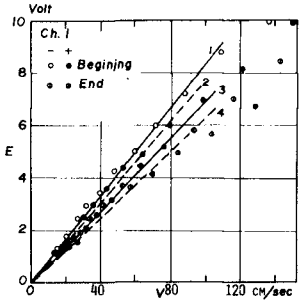

Fig. 10 Calibration for Periodic Wave Tests (Series I)

2.4 Test Schedule

Testing was first performed on periodic waves in order to compare laboratory measurement with the theories that are felt to be most applicable. Measurements were made simultaneously with the propeller meter and the hot film anemometer in order to also compare results between these two measurement methods. The test schedule was then organized into the topics of instrument calibration, comparison between instruments, comparison between measurements and periodic wave mathematical predictions, and comparisons between measurements in random waves and predictions from periodic wave theory. The tests were intended to sample a wide range of wave height and period as indicated in Table 1. Some measurements were made by Jensen (5) using the propeller meter only. These measurements concentrated in the area between the wave trough and the wave crest.

Table 1 Wave Conditions for Periodic Waves Tested

Wave height H (cm)	Wave period T (sec)	Ursell number U	Index in ref.(1)	Probe Position z (cm)		
				Series I	Series II	Series III
110.0	2.50	1.89		-122.0	-61.0	-30.5
83.5	2.50	0.72		--	--	-30.5
38.4	2.50	0.65		-122.0	-61.0	--
82.6	2.07	0.78	8-C	-122.0	-61.0	-30.5
28.7	2.07	0.18	8-A	-122.0	-61.0	--
40.5	1.47	0.10	9-C	-122.0	-61.0	--
14.3	1.47	0.024	9-A	-122.0	-61.0	--
61.3	4.61	5.4	6-A	-122.0	-61.0	--
52.4	3.28	1.72	7-A	-122.0	-61.0	--
104.9	3.28	4.02	7-B	-122.0	-61.0	--

*Note Series I and II were repeated twice for two propeller orientations: horizontal and vertical. In Series III, hot film only was operated. Another series was tested by Jensen with the propeller meter at several vertical positions between the wave trough and crest.

Two wave spectra were used for the random wave tests, wherein the water velocity measurements were made primarily with the hot film anemometer. The spectra are shown in Figs. 11 and 12.

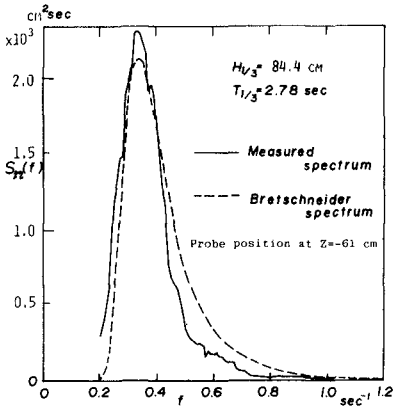

Fig. 11 Experimental Wave Spectrum I

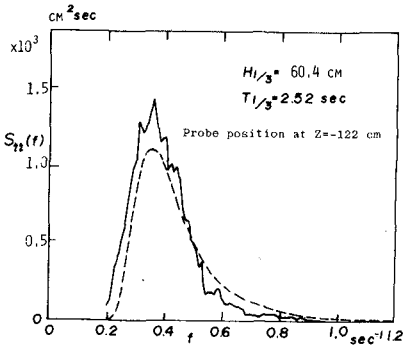

Fig. 12 Experimental Wave Spectrum II

On the figures the random wave parameters were obtained from the direct reduction of zero upcrossing wave heights and periods. The wave trains were approximately 160 secs. long and they contained approximately 60 zero upcrossing waves each. The range of parameters for the individual waves in spectrum I are shown in Fig. 13. The periodic wave conditions are shown with triangles on Fig. 13 and the random waves are solid dots. Figure 14 gives the parametric variations for spectrum II.

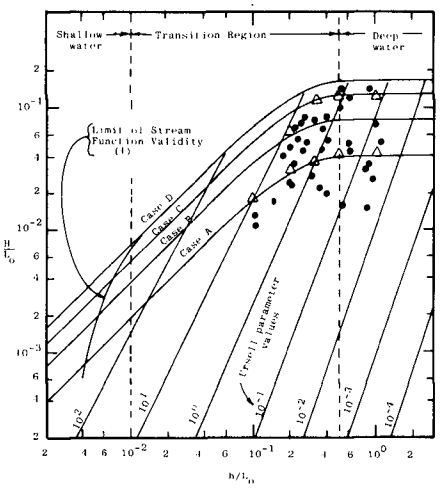

Fig. 13 Range of Periodic Waves, Δ, Individual Random waves, ● , for Spectrum I.

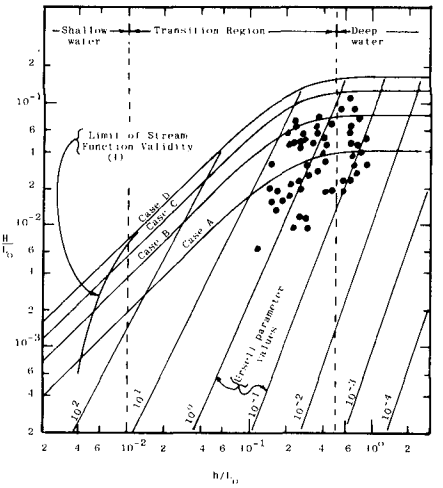

Fig. 14 Range of Individual Random Waves for Spectrum II.

2.5 Data Analysis

The accuracies of all experimental studies are particularly dependent on the care taken and the methods used to analyze the data. The intent of this section is to explain the methods used herein and to point out problem features.

The hot film anemometer turned out to be a versatile and excellent instrument for this study. However, we did not realize until after the study that the entire velocity vector, as a function of time, at a point, can be measured with it as reviewed in (12) and clarified in (6). It is suggested that for future experimental studies dealing with wave theory verification that the entire vector be thus determined. However, wake problems are still bothersome wherein one sensor can shield the other, or the mounting itself might shield both sensors, as seems to have been the case in (12) for some flow directions. Anyway, the maximum horizontal and vertical velocities are very important in design and they are featured in this study.

The propeller meter output is sometimes difficult to read if the impulses are too close. The recording media must be run at sufficient

speed for adequate resolution. As previously stated, the propeller meter is very sensitive to flow direction and for this study only, the data were utilized where it was felt the flow direction was parallel with the propeller axis.

2.5.1 Periodic waves

A sample record for periodic waves is shown in Fig. 15, which is a photocopy of the actual visicorder recording. The record shows, from the top, water surface elevation, nonlinear outputs from Sensors 1 and 2, linearized outputs from Sensors 1 and 2, and the output from the propeller, the orientation of which is horizontal for this record.

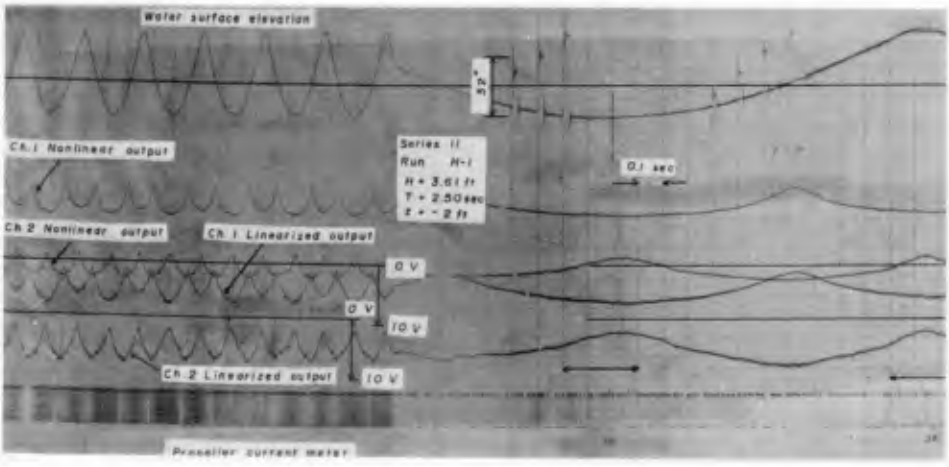

Fig. 15 Sample Record of Periodic Wave

It is seen that the pulses from the propeller are dense at a wave crest and trough. The maximum frequency, n, of the pulses was determined as the mean frequency over a period of from 0.3 to 0.2 seconds under the wave crests and troughs. The maximum velocities were reduced with the conversion relation given on Fig. 8. The linearized output from Sensor 1 shows maxima at wave crests and troughs, while that from Sensor 2 shows minima. In the same way, the output from Sensor 2 shows maxima at wave nodes approximately, while that from the other sensor shows minima. Thus, variations of the output from Sensors 1 and 2 correspond to those of the magnitude of the theoretical horizontal and vertical velocity component, respectively. However, it should be noted that the minimum voltage is not zero, while wave theories predict that the minimum magnitude of each velocity component is zero. This is caused by the effect of the parallel velocity component. Each cylindrical film sensor output voltage is due to both the normal and transverse velocity components with respect to the sensor axis. When the normal velocity component is a minimum there can still be a sizable parallel component that will create a voltage reading. From the records, the following maximum velocities were reduced from the maximum output voltage using the corresponding calibration curves for each sensor.

u_+: the horizontal velocity beneath a wave crest

u_-: the horizontal velocity beneath a wave trough

w_+: the vertical velocity when the water surface crosses the still water level upward

w_-: the vertical velocity when the water surface crosses the still water level downward

2.5.2 Random waves

A typical record for the random wave tests is shown in Fig. 16. Generally, the maxima of the output voltage from Sensor 1 appear beneath the wave crests and troughs where the output from Sensor 2 shows its minima. The maxima of Sensor 2 appear at the wave nodes while the output from Sensor 1 shows the minima. These aspects are clearly seen for large waves and have the same general charcteristics as observed in the periodic wave tests. Hence, the maximum values of horizontal and vertical velocity components in a random wave train were processed in the same way that was used for the periodic wave tests.

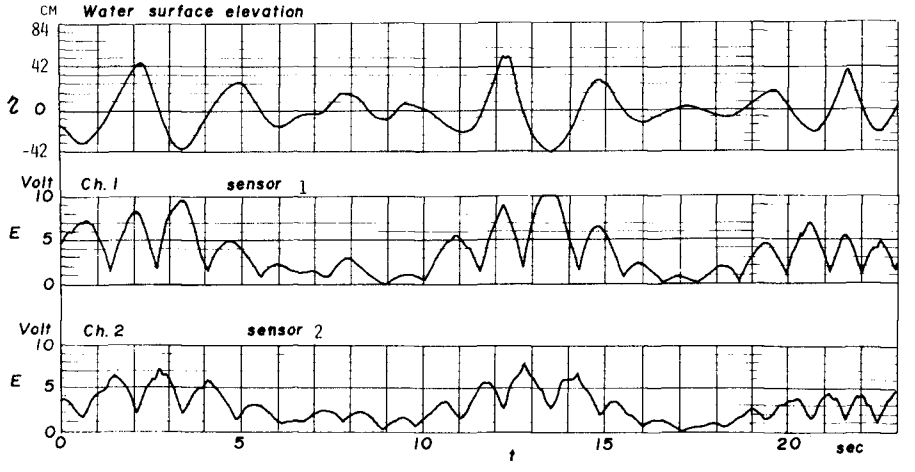

Fig. 16 Sample Record of Random Wave Test (Spectrum II, Z = -61 cm)

3.0 RESULTS

This section will first compare the results from the hot film anemometer to those from the propeller meter. Periodic wave theory predictions will then be compared to measurements in periodic waves, followed by measurements in random waves.

The measurements made with the hot film anemometer compared very favorably with the propeller meter. Correlation curves were obtained and the coefficients calculated for various wave conditions. The results are displayed in Table 2.

Table 2 Correlation Coefficients between propeller meter and hot film anemometer for various conditions

Wave Type	Probe Position (cm)	Velocity Measured	Correlation Coefficient
Periodic	-61	$u_{+,-}$	0.993
"	-61	$w_{+,-}$	0.974
"	-122	$u_{+,-}$	0.991
"	-122	$w_{+,-}$	0.947
Spectrum I	-61	$u_{+,-}$	0.983
"	-61	$w_{+,-}$	0.976
Spectrum II	-61	$u_{+,-}$	0.952
"	-61	$w_{+,-}$	0.970

For comparing predictions vs. measurements for velocities, the error is defined as

$$r = \frac{(u)_{measured} - (u)_{predicted}}{(u)_{predicted}} \qquad (2)$$

where u stands for $u_{+,-}$ or $w_{+,-}$.

In order to compare linear theory to measurements of fairly high finite amplitude waves, it is necessary to use a ficticious water depth so that the wave crests and troughs for linear theory will occur at the same elevations as the measurements. This condition is shown in Fig.17. An example of a few measurements vs. theory, for an intermediate water depth wave, is shown in the usually accepted way in Fig. 18. All of the errors for the periodic wave tests were calculated according to Eq. 2 for each of the theories and they are summarized in Table 3. Wave steepness A, B and C refer to the Dean classification with $H_A = 1/4\ H_b$ and $H_c = 3/4\ H_b$, etc.

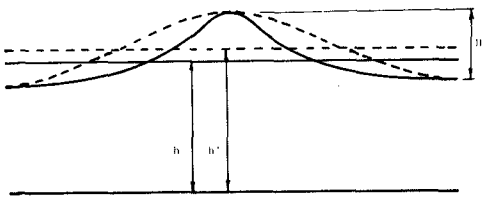

Fig. 17 Finite Amplitude vs. Airy Wave

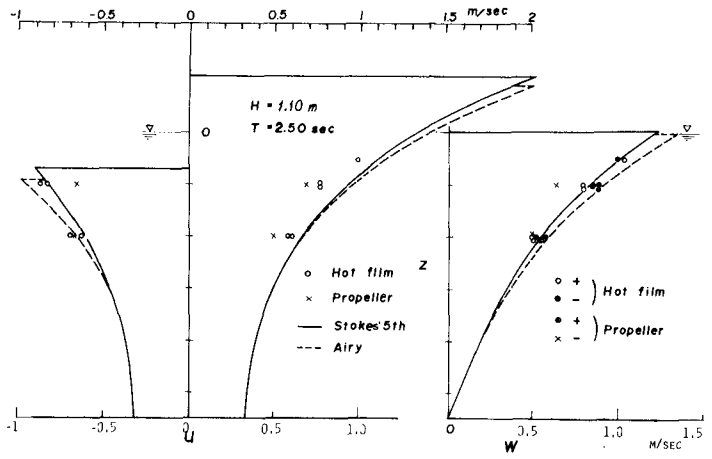

Fig. 18 Comparison with Theory (run 1)

Table 3 Error Mean and Standard Deviation for Periodic Waves

Item	Elevation	Wave Steepness	Theory	u_+	u_-	w_+	w_-
Mean	Above Trough	A	Dean's ψ	-.094			
			Airy	-.075			
		B	Dean's ψ	-.040			
			Airy	-.040			
		C	Dean's ψ	-.072			
			Airy	-.077			
		ALL	Dean's ψ	-.061			
			Airy	-.063			
	-61 cm		Stokes 5th	-.043	+.196	+.056	-.031
			Airy	-.040	+.112	+.016	-.070
	-122 cm		Stokes 5th	-.032	+.110	-.101	-.071
			Airy	-.025	+.059	-.126	-.098
Standard Deviation	Above Trough	A	Dean's ψ	.097			
			Airy	.106			
		B	Dean's ψ	.083			
			Airy	.071			
		C	Dean's ψ	.063			
			Airy	.069			
		ALL	Dean's ψ	.084			
			Airy	.079			
	-61 cm		Stokes 5th	.106	.089	.115	.111
			Airy	.116	.120	.117	.095
	-122 cm		Stokes 5th	.201	.123	.211	.122
			Airy	.209	.133	.213	.110

The means of the relative error show that the horizontal velocity beneath the wave crests are three to four percent smaller and those beneath the wave troughs are 10 to 20 percent larger than those predicted from the theories. On the other hand, the measured vertical velocities, in general, are smaller than the theoretical predictions for both w_+ and w_-. The standard deviations vary from 0.1 to 0.2 at the level of -122 cm and they are about 0.1 at the level of -61 cm. According to the mean and standard deviations listed, there was no significant difference for the wave theory used: higher order wave theories or Airy theory. Hence, for the convenience of the remainder of the computation herein, Airy theory is used to predict the velocities of each discrete wave in a random wave train. This conclusion was also reached in (4).

The results from measurements vs. predictions for the two random waves were quite encouraging for the continued use of the Airy theory, even above the wave troughs. For both spectra tested, the individual zero upcrossing wave height distributions were closely approximated by the Rayleigh distribution as shown in Fig. 19. In addition, the maximum horizontal velocities under the wave crests were closely approximated by the Rayleigh distribution as shown in Fig. 20.

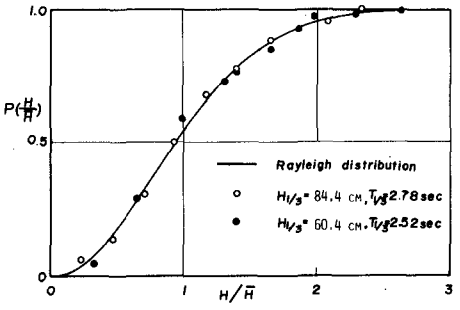

Fig. 19 Random Wave Height Distribution

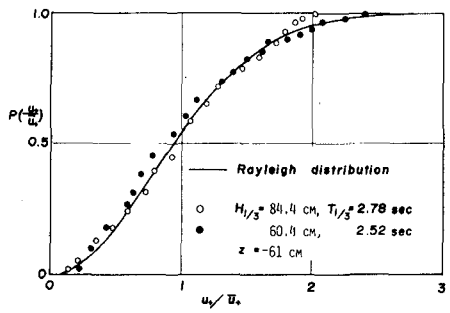

Fig. 20 Probability Distribution of Horizontal Velocities Beneath the Wave Crests.

The comparison between Airy theory and measurements for the horizontal velocities is shown in Fig. 21 for the vertical velocities, for z = -61 cm. The scatter appears to be reasonable and was treated statistically as will be explained. For vertical velocities, the correlation was 0.934 for w_- and 0.638 for w_+, with the plots looking much like Fig. 21.

Samples of how the errors were plotted on normal probability paper are shown in Figs. 22 and 23. The figures show that as the sample size is reduced by focusing on the smaller number of larger waves (i.e. $H_{1/10}$ vs. $H_{1/3}$) the standard deviation of the errors is reduced! This means that the factor of safety can be made smaller for calculating the kinematics for the larger waves, as will be shown. The total sample sizes were from 60 to 70 waves.

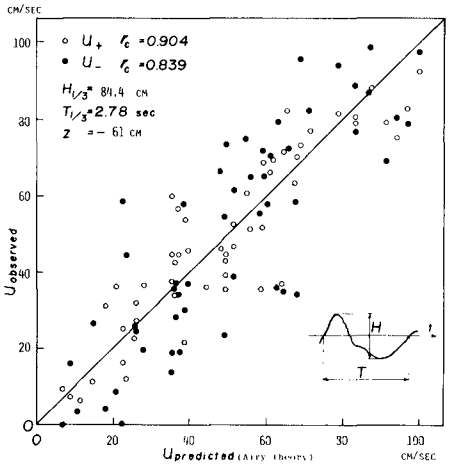

Fig. 21 Comparison Between Predicted and Observed Horizontal Velocities for Random Waves

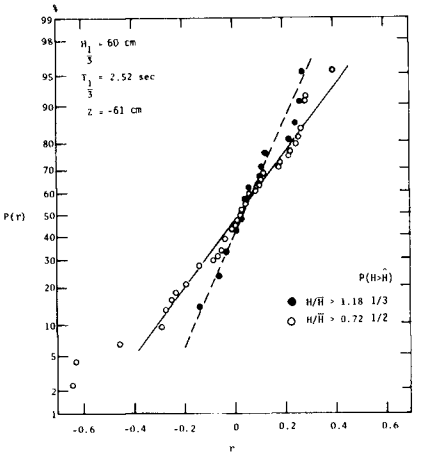

Fig. 22 Probability Distribution of Relative Errors for Horizontal Velocities Under Wave Crests

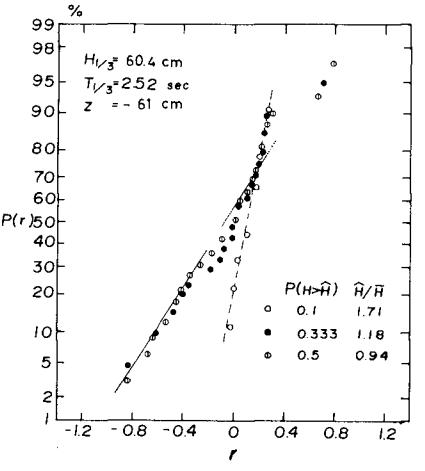

Fig. 23 Probability Distribution of Relative Errors for Vertical Velocities

The normal distribution hypothesis was checked with the chi square test and it was found that almost all populations passed the test at a significance level of 95%. The populations of $H_{1/10}$ were not checked because they were quite small. In this manner, the mean and standard deviations of the errors between the measurements and Airy theory were compared for various fractions of the wave height populations for sensor position below the wave troughs. The results are shown in Table 4. It is seen that the standard deviations of the errors clearly reduced markedly as the height of the samples were restricted to ever increasing wave heights. The data between wave troughs and crests were treated similarly, with similar trends resulting. However, the means were closer to zero and the standard deviations were even smaller, as reviewed in the next section.

Table 4 Errors as Functions of Wave Height Fraction

Spectrum	Sensor Position (Z)	Wave Height Fraction $P(H>\hat{H})$	error mean (r)				error standard deviation (σ_r)			
			u_+	u_-	w_+	w_-	u_+	u_-	w_+	w_-
I	-61 cm	.10	-.05	-.01	-.17	.06	.09	.14	.33	.11
		.33	.00	.04	-.02	.04	.15	.23	.36	.12
		.50	-.03	.03	.04	-.01	.22	.29	.39	.18
		.67	.00	.03	.08	-.01	.26	.29	.48	.17
		.90	.02	.04	.09	-.02	.34	.45	.53	.17
	-122 cm	.10	-.17	.08	-.24	-.10	.09	.12	.28	.09
		.33	-.17	.07	-.06	-.10	.26	.37	.32	.09
		.50	-.09	.13	-.05	-.13	.28	.38	.39	.16
		.67	-.06	.11	.02	-.06	.33	.39	.46	.16
		.90	-.04	.12	.09	-.07	.46	.51	.65	.20
II	-61 cm	.10	.10	-.03	.01	-.09	.14	.19	.31	.17
		.33	.06	.04	.00	-.08	.13	.30	.42	.17
		.50	.01	.08	-.03	-.09	.21	.37	.41	.17
		.67	.05	.15	-.01	-.03	.34	.51	.49	.33
		.90	.07	.16	.06	-.04	.37	.55	.51	.33
	-122 cm	.10	-.04	.01	-.02	-.20	.09	.22	.14	.11
		.33	-.03	.05	.08	-.13	.15	.29	.36	.12
		.50	-.07	.16	-.15	-.15	.19	.31	.34	.21
		.67	-.03	.17	-.09	-.14	.36	.53	.39	.18
		.90	-.01	.22	-.06	-.18	.43	.70	.48	.29

4.0 DISCUSSION

The comparisons between the measurements made with the hot film anemometer and the propeller meter were very good. From this it can be concluded that the laboratory and experimental techniques concerning the instruments were excellent. Experimentation in periodic waves showed fairly good agreement between measurements and periodic wave theory. This was done in order to compare with the work of others and as another

step in verifying the laboratory method for measuring wave velocities. Since the agreement between measurements and predictions was quite good it is felt that the measurements then made within random waves would be quite reliable.

The laboratory data indicate that the large random waves have the smaller standard deviations of errors between theoretical predictions and measurements. In addition, the variation of the means and the standard deviations are about the same whether one utilizes finite amplitude wave theories or the Airy wave theory. The hot film anemometer is reliable and relatively handy to use *providing* proper calibration techniques are utilized. There is still a wake problem which can be minimized with the proper orientation of the hot film anemometer.

Thus, according to the measurements made for this study, it is reasonable to use periodic wave theory to predict the particle kinematics in large waves, given that a complete dynamic analysis of the structure is not necessary. Thus, the designer may be interested in predicting *maximum* values (e.g. maximum horizontal velocity) *given* the design wave. The errors in this work were distributed normally so that two standard deviations added to the mean will include 97.7% of the population and three standard deviations will include 99.9%. Considering the errors between laboratory random waves and actual storm waves, it would seem to be prudent to use the 3σ level.

Now consider Eq. 2 for error definition and let r_{u+} be the error under the crest for the maximum horizontal velocity. In the field, the actual maximum horizontal velocity under the crest for the *design* wave (given that it occurs) will also be in error with design predictions. Let this occurrence be designated as

$$\varepsilon_{u+} = \frac{u_a - u_p}{u_p} \tag{3}$$

where u_a is the actual maximum horizontal velocity. Now, let $u_a = u_d$, the design value for the maximum horizontal velocity, and solve for it from Eq. 2

$$u_d = u_p\ (1 + \varepsilon_{u+}) \text{ or} \tag{4}$$

$$u_d = u_p .\ \ FS \tag{5}$$

where u_p, again, is the value predicted from Airy theory and FS is the factor of safety. The error value must now be estimated. We propose

$$\varepsilon_{u+} = \bar{r}_{u+} + 3\sigma \tag{6}$$

where the overbar indicates the average value, and the values of FS determined therefrom are displayed in Fig. 24. The factors of safety for the spectrum conditions were calculated for the $H_{1/10}$ conditions.

Since the larger waves in the random series have the smallest standard deviation for the errors and a relatively small variation in the means, it is concluded that it is reasonable to use periodic theory (in

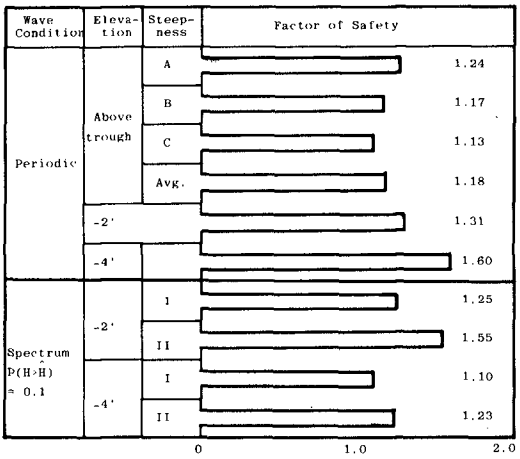

Fig. 24 Factor of Safety for u_+ for Airy Theory

fact Airy wave theory) to predict the conditions in large waves at sea providing an appropriate factor of safety is used. An example is shown here for u_+. Similar safety factors can be developed for other wave parameters at the discretion of the designer.

5.0 ACKNOWLEDGEMENTS

Some of the work in this research was supported by the National Science Foundation Grant No. ENG76-16423, on the section regarding wave kinematics and circulation in a closed system wave flume. Dr. Tokuo Yamamoto provided valuable comments at the beginning of the work. The authors are indebted to Prof. C. K. Sollitt and Mr. Robert Jensen for use of the data on horizontal velocity measurements above the trough, which were collected from Mr. Jensen's M. S. Thesis.

REFERENCES

1. Dean, R.G., "Evaluation and Development of Water Wave Theories for Engineering Application," Special Report No. 1, U.S. Army, Coastal Engineering Research Center, Vol. ii, 1974, p. 534.
2. Grace, R.A. and R.T. Rocheleu, "Near-Bottom Velocities Under Waikiki Swells," James K.K. Look Laboratory of Oceanographic Engineering, University of Hawaii, Technical Report No. 31, 1973, p. 55.
3. Hudspeth, R.T., D.F. Jones and J.H. Nath, "Design of Hinged Wavemakers for Random Waves," 16th International Conference on Coastal Engineering, Hamburg, September 1978.
4. Iwagaki,Y., T. Sakai and H. Ishida, "Correlation of Water Particle Velocity with Water Level Variation for Irregular Waves," Coastal Engineering in Japan, Vol. 16, 1973, pp. 19-28.

4. Iwagaki, Y., T. Sakai and H. Ishida, "Correlation of Water Particle Velocity with Water Level Variation for Irregular Waves," Coastal Engineering in Japan, Vol. 16, 1973, pp. 19-28.

5. Jensen, R., "Finite Amplitude Deep Water Wave: a comparison of theoretical and experimental kinematics and dynamics," Thesis for Master of Ocean Engineering Degree, Oregon State University, June 1979.

6. Kobune, K., "Random Wave Velocity Field from Periodic Theory," Thesis for the Degree of Civil Engineer, Oregon State University, June 1978, presented December 1977.

7. Lee, A., C. A. Grated and T.S. Durrani, "Velocities Under Periodic and Random Waves," Proceedings of 14th Conference on Coastal Engineering, 1974, pp. 558-574.

8. Nath, J. H., "Drift Speed of Buoys in Waves," Proceedings of 16th International Conference on Coastal Engineering, Hamburg, 1978.

9. Reid, R.O., "Correlation of Water Level Variation with Wave Forces on a Vertical Pile for Nonperiodic Waves," Proceedings of 4th International Conference on Coastal Engineering, 1958, pp.749-786.

10. Tsuchiya, Y. and M. Yamaguchi, "Horizontal and Vertical Water Particle Velocities Induced by Waves," Proceedings of 14th International Conference on Coastal Engineering, 1974, pp. 555-568.

11. Ursell,F., "The Long-Wave Paradox in the Theory of Gravity Waves," Proceedings of the Cambridge Philosophical Society, Vol. 49, 1963, pp. 685-694.

12. Van Dorn, W. G. and S. E. Pazan, "Laboratory Investigation of Wave Breaking, Part III: deep water waves," Advanced Ocean Engineering Laboratory Report No. 71, Scripps Institution of Oceanography, University of California, San Diego, 1975, p. 105.